Modelling ICCD Experiments for Sawtooth Control in JET

J. P. Graves*, W. A. Cooper*, S. Coda*, L.-G. Eriksson†, T. Johnson** and JET-EFDA Contributors‡

*Centre de Recherches en Physique des Plasmas, Association EURATOM-Confederation Suisse, EPFL, 1015 Lausanne, Switzerland (jonathan.graves@epfl.ch)
†Association EURATOM-CEA, CEA/DSM/DRFC, CEA-Cadarache, F-13108 St. Paul lez Durance, France
**Association Euratom-VR, KTH, SE-100 44 Stockholm, Sweden
‡Proc. 20th IAEA Conference, Vilamoura, Portugal, 2004.

INTRODUCTION

The motivation of this work is to characterise a model for the distribution function of ICRH populations which can easily be employed in stability codes. The model described here has already been incorporated in the 3D equilibrium code VMEC [1], and 3D fluid stability code TERPSICHORE [2]. Furthermore, the model lends itself to relatively straightforward semi-analytical calculations of macroscopic stability in tokamaks, and in particular the stability of the internal kink mode in the presence of ICRH ions. Despite the apparent simplicity of the model, it will be seen that the three radially dependent parameters in the distribution function enable the recovery of the salient features of the SELFO [3] simulations. In this work an attempt is made to parameterise the distribution function for SELFO simulations of the important JET discharge 58934 [4], shown here in Fig. 1. This discharge demonstrates that an off-axis ion cyclotron resonant surface, with phasing to enable ion cyclotron current drive (ICCD), can destabilise (shorten period of) sawteeth even when the sawteeth are initially stabilised by trapped energetic RF ions in the core. Hence, in the latter part of the discharge two resonant surfaces co-exist. It is the sum of these two populations that ultimately require modelling in order to ascertain the internal kink mode stability.

MODEL ICRF DISTRIBUTION FUNCTION

The distribution of particles F depend only the constants of the particle motion: energy $E = mv^2/2$, magnetic moment $\mu = mv_\perp^2/B$ and flux surface label r. Here $v_\perp$ is the velocity perpendicular to the magnetic field. The distribution is written in terms of a bi-Maxwellian in $v_\parallel$ and $v_\perp$:

$$F = \left(\frac{m}{2\pi}\right)^{3/2} \frac{n_c(r)}{T_\perp(r) T_\parallel^{1/2}(r)} \exp\left[-\frac{\mu B_c}{T_\perp(r)} - \frac{|\mathscr{E} - \mu B_c|}{T_\parallel(r)}\right].$$

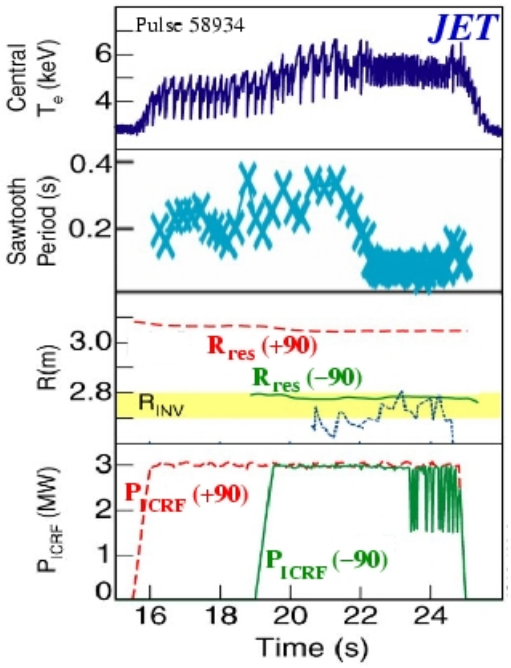

FIGURE 1. Pulse 58934 in JET [4], plotting the electron temperature, sawtooth period, sawtooth inversion radius R_{inv} and first harmonic H cyclotron resonance layer R_{res}(H) for $+90^\circ$ and -90° phasings, and heating power for the two antennas.

Here in general the critical field strength B_c can in principle also depend on the flux label r, but a constant B_c is usually more appropriate. In the above n_c is the local density evaluated where $B = B_c$ on the flux surface r. Taking the zero'th moment of the distribution function yields the variation of the density with respect to B:

$$n(r,B) = n_c N_B$$

where

$$N_B = \frac{T_{\perp a}}{T_\perp} \quad \text{for} \quad B > B_c \quad \text{and}$$

$$N_B = \frac{T_{\perp a}}{T_\perp} + \frac{T_{\perp b} - T_{\perp a}}{T_\perp} \left(\frac{T_\perp}{T_\parallel} \right)^{1/2} \left(\frac{B_c - B}{B_c} \right)^{1/2} \quad \text{for } B < B_c, \text{ and}$$

$$T_{\perp a} = T_\perp \left[\frac{B_c}{B} + \frac{T_\perp}{T_\parallel} \left(1 - \frac{B_c}{B} \right) \right]^{-1} \quad \text{and} \quad T_{\perp b} = T_\perp \left[\frac{B_c}{B} - \frac{T_\perp}{T_\parallel} \left(1 - \frac{B_c}{B} \right) \right]^{-1}.$$

Denoting the flux surface average with angular brackets we can identify

$$n_c = \langle n \rangle \, G(r) \quad \text{and} \quad G = (2\pi)^2 \left[\int_0^{2\pi} d\theta \int_0^{2\pi} d\phi \, N_B \right]^{-1}$$

where G assumes the role of normalising a distribution function defined in terms of $\langle n \rangle$, and θ and ϕ are the poloidal and toroidal angles respectively.

Now, taking second moments of the distribution function it can be shown that

$$P_{\|} = n_c T_{\|} H_{\|} \text{ and } P_{\perp} = n_c T_{\perp} H_{\perp},$$

where for $B > B_c$:

$$H_{\|} = \left(\frac{T_{\perp a}}{T_{\perp}}\right) \text{ and } H_{\perp} = \left(\frac{T_{\perp a}}{T_{\perp}}\right)^2,$$

while for $B < B_c$:

$$H_{\|} = \left[\frac{T_{\perp a}}{T_{\perp}} + \left(\frac{T_{\perp}}{T_{\|}}\right)^{3/2} \left(\frac{B_c - B}{B_c}\right)^{3/2} \left(\frac{T_{\perp b} - T_{\perp a}}{T_{\perp}}\right)\right]$$

$$H_{\perp} = \left[\left(\frac{T_{\perp a}}{T_{\perp}}\right)^2 + \left(\frac{T_{\perp}}{T_{\|}}\right)^{1/2} \left(\frac{B_c - B}{B_c}\right)^{1/2} \left\{\frac{T_{\perp b} - T_{\perp a}}{2T_{\perp}} \left(\frac{B}{B_c}\right) + \frac{T_{\perp b}^2 - T_{\perp a}^2}{T_{\perp}^2}\right\}\right].$$

PARAMETERISING THE DISTRIBUTION FUNCTION

Here 3D data files from the SELFO simulations of n, $P_{\perp}$ and $P_{\|}$ are used to identify the three radially dependent parameters of the model distribution function. In particular, in the following, the LHS of the equations correspond to the parameters in the model, and the RHS of the equations are the quantities from the SELFO simulations:

$$n_c(r) = n(R_c, Z) \ , \ T_{\perp}(r) = \frac{P_{\perp}(R_c, Z)}{e\, n(R_c, Z)} \text{ and } A(r) \equiv \frac{T_{\perp}(r)}{T_{\|}(r)} = \frac{P_{\perp}(R_c, Z)}{P_{\|}(R_c, Z)}.$$

Now, since the heating is approximately located on a vertical line through the plasma cross section we can resolve the minor radius on the LHS of the equations through $r^2 = Z^2 + (R_c - R_0)^2$ with Z defining the distance along a vertical chord $R = R_c$.

Where there are two resonant surfaces the problem is treated upon assuming the sum of model distributions. Hence there are now six radially dependent parameters to resolve namely $n_c(r)$, $T_{\perp}(r)$ and $A(r)$ for the two distributions. The problem has been treated upon exploitation of simulations with off-axis heating alone. This enabled identification of the three functions for off-axis heating, and thus when employed in conjunction with the parameters obtained with on-axis heating alone, provided a first guess for the distribution function for the combined heating case. The six functions were then normalised iteratively to provide a best parameter fit of the 3D plots of the density, parallel pressure and perpendicular pressure. The result of such a procedure for the case at hand, i.e. JET discharge 58934, is shown in Fig. 2. Plotted are the radial profiles of $n_c(r)$, $T_{\perp}(r)$ and $A(r)$ for the two coexisting resonant RF populations, and the resulting flux surfaced averaged density and parallel pressure. The latter two are compared favourably with the corresponding SELFO data. Finally, Fig. 3 shows the density and parallel pressure over the entire poloidal cross section. Peaks in the density and pressure result from the localised deposition of the RF heating, and are again seen to recover the salient features of the SELFO data.

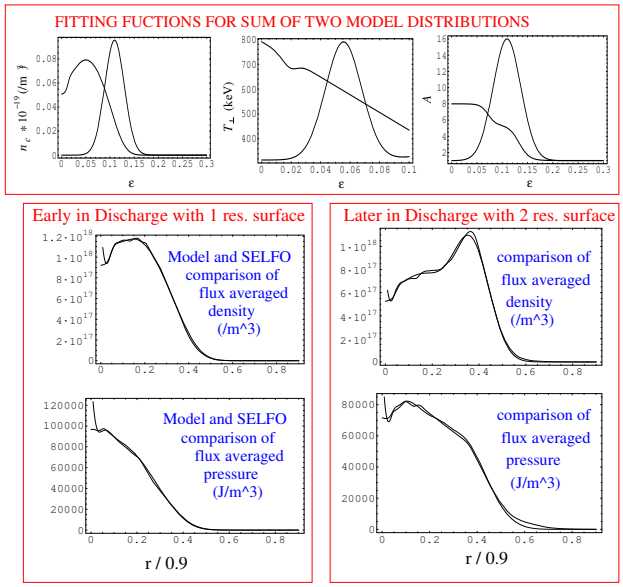

FIGURE 2. Plots of $n_c(r)$, $T_\perp(r)$ and $A(r)$ for the two distributions to reproduce the SELFO simulations of the latter part of discharge 58934. Also shown are SELFO and model comparisons of the resulting flux averaged density and pressure profiles.

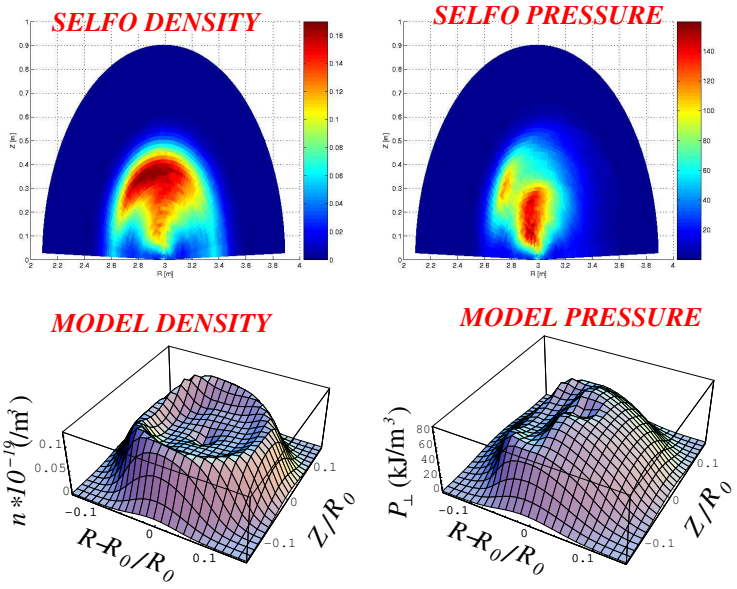

FIGURE 3. A comparisons between the analytical model and SELFO of the density and perpendicular pressure surfaces for the parameters in Fig. **??**

FAST ION CONTRIBUTION TO STABILITY OF INTERNAL KINK MODE

Presented here are the equations required to assess the stability of the internal kink mode for the model distribution function. It is assumed that the fast ion pressure is much

smaller than the core pressure, and thus does not significantly modify the equilibrium. The opposite limit will be treated elsewhere. The ideal growth rate is identified with the normalised potential energy terms:

$$\frac{\gamma}{\tau_A} = -\frac{\pi}{s_1}(\delta\hat{W}_I + \delta\hat{W}_A + \delta\hat{W}_k)$$

with $\delta\hat{W}_I$ the ideal MHD, $\delta\hat{W}_A$ the adiabatic contribution due to pressure anisotropy, and $\delta\hat{W}_k$ the non-adiabatic (kinetic) contribution

$$\delta\hat{W}_k = -\frac{3\varepsilon_1^{-1/2}}{\pi 2^{3/2}}\left(\frac{2\mu_0}{B_0^2}\right)\int_0^{r_1} dr\left(\frac{r}{r_1}\right)^{3/2}\left(\frac{2}{1+\kappa}\right)^2 F_k(r),$$

with κ the elongation and

$$F_k(r) = \int_0^1 dk^2 \frac{F_q^2 J^t}{F_1\left(\frac{2}{1+\kappa}\right) + 2sF_2 - \zeta\left(\frac{1}{4q^2} + F_3\right)},$$

and J^t is determined by the model distribution:

$$J^t = \frac{(n_c T_\perp A^{1/2})' - \frac{5}{2}\left(\frac{n_c T_\perp A^{1/2}|\varepsilon_c + \varepsilon(2k^2-1)|}{1+A|\varepsilon_c+\varepsilon(2k^2-1)|}\right)A'}{(1+A|\varepsilon_c+\varepsilon(2k^2-1)|)^{5/2}},$$

where ε_c defines the resonant surface location through the identity $B_c = B_0/(1+\varepsilon_c)$.

The following is a reasonable fit of F_q:

$$F_q = 2E(k^2) - K(k^2) + 4[1-q(r)][E(k^2) + (k^2-1)K(k^2)]$$

where E and K are compete elliptic integrals of the second and first kinds. Furthermore,

$$F_1 = 2E(k^2) - K(k^2), F_2 = 2E(k^2) + 2(k^2-1)K(k^2),$$

$$F_3 = \frac{4}{3}[(2k^2-1)E(k^2) + (1-k^2)K(k^2)]$$

and $\zeta = -\frac{2R\mu_0}{B^2}\frac{dP}{dr}q^2$ is 'ballooning' parameter, and P the plasma pressure.

The anisotropic term $\delta\hat{W}_A$ is the sum of trapped (t) and passing (p) contributions given by:

$$\delta\hat{W}_A^{t,p} = -\frac{3\varepsilon_1^{-1/2}}{\pi 2^{3/2}}\left(\frac{2\mu_0}{B_0^2}\right)\int_0^{r_1} dr\left(\frac{r}{r_1}\right)^{3/2}\left(\frac{2}{1+\kappa}\right)F_A^{t,p}(r),$$

$$F_A^t(r) = \int_0^1 dk^2 \frac{2G_1^t + G_2^t}{[1+\varepsilon(2k^2-1)]^{5/2}}J^t \quad \text{and} \quad F_A^p(r) = \int_0^1 dk^2 \frac{2G_1^p + G_2^p}{[k^2+\varepsilon(2-k^2)]^{5/2}}J^p,$$

with

$$J^p = \frac{k^5\left[(n_c T_\perp A^{1/2})' - \frac{5}{2}\left(\frac{n_c T_\perp A^{1/2}|k^2\varepsilon_c+\varepsilon(2-k^2)|}{k^2+A|\varepsilon_c k^2+\varepsilon(2-k^2)|}\right)A'\right]}{\left(k^2+A|\varepsilon_c k^2+\varepsilon(2-k^2)|\right)^{5/2}}$$

and G_1^t, G_2^t, G_1^p, G_2^p are given in Ref. [6]:

$$\begin{aligned}
G_1^t &= \left(\frac{2\varepsilon}{3}\right)\left[(1-k^2)K(k^2)+(2k^2-1)E(k^2)\right], \\
G_2^t &= 2E(k^2)-K(k^2)+\left(\frac{2\varepsilon}{3}\right)\left[(1-4k^2)K(k^2)+(8k^2-4)E(k^2)\right], \\
G_1^p &= \left(\frac{2\varepsilon}{3k^2}\right)\left[(2-k^2)E(k^2)-2(1-k^2)K(k^2)\right] \\
&- \left(\frac{2\varepsilon^2}{15k^4}\right)\left[(4k^4-12k^2+8)K(k^2)+\left(7k^4+8k^2-8\right)E(k^2)\right], \\
G_2^p &= 2E(k^2)+(k^2-2)K(k^2)-\left(\frac{2\varepsilon}{3k^2}\right)\left[\left(3k^4-8k^2+8\right)K(k^2)+\left(4k^2-8\right)E(k^2)\right] \\
&- \left(\frac{2\varepsilon^2}{15k^4}\right)\left[16(k^4-3k^2+2)K(k^2)-2(k^4-16k^2+16)E(k^2)\right].
\end{aligned}$$

CONCLUSIONS

The work presented here provides a means of assessing the stability of the internal kink mode with ICRH distributed ions. It will also enable analysis of the impact of the fast ions on the equilibrium [1, 2]. Calculations of the fast ion contribution to ideal stability $\delta\hat{W}_A+\delta\hat{W}_k$ indicate that the internal kink mode is strongly stabilised with the single resonant surface close to the magnetic axes. However, calculations with the two resonant surfaces reveal that the contribution of the ICRH population to ideal stability is negligible. For the latter case the net effect of the ICRH population on sawteeth is thus felt predominantly through the effect of ICCD on the evolution of the safety factor. Sawtooth control techniques in ITER will employ localised current drive in conditions where there is strong ideal stabilisation from alpha particles.

ACKNOWLEDGMENTS

This work was partly funded by the Fonds National Suisse de la Recherche Scientifique and EURATOM.

REFERENCES

1. W.A. Cooper, J P Graves *et al* Nucl. Fusion **46**, 683 (2006).
2. W.A. Cooper, J P Graves *et al* Fusion Science and Technology **50**, 245 (2006).
3. J. Hedin *et al* Nucl. Fusion **42**, 527 (2002).
4. L-G. Eriksson, *et al*, Phys. Rev. Lett. **92**, 235004 (2004).
5. J. P. Graves *et al*, Phys. Rev. Lett. **84**, 1204 (2000).
6. J. P. Graves *et al* Phys. Plasmas **10**, 1034 (2003).